J. Biochem. 2009;146(5)733–742
doi:10.1093/jb/mvp120

Differential Assembly Properties of *Escherichia coli* FtsZ and *Mycobacterium tuberculosis* FtsZ: An Analysis Using Divalent Calcium

Richa Jaiswal and Dulal Panda*

School of Biosciences and Bioengineering, Indian Institute of Technology, Bombay, Powai, Mumbai – 400076, India

Received July 7, 2009; accepted July 25, 2009; published online August 5, 2009

The assembly of FtsZ is considered to be a fundamental process during the bacterial cytokinesis. We used several complimentary techniques to probe the assembly of recombinant *Escherichia coli* FtsZ (*Ec*FtsZ) and *Mycobacterium tuberculosis FtsZ* (*Mtb*FtsZ) proteins *in vitro*. As documented earlier, *Ec*FtsZ was found to polymerize at much faster rate than *Mtb*FtsZ. Interestingly, we found that *Mtb*FtsZ produced higher sedimentable polymerized mass than that of the *Ec*FtsZ and that *Mtb*FtsZ formed thicker protofilaments than that of the *Ec*FtsZ. The results indicated that the *Ec*FtsZ polymers are more labile than the *Mtb*FtsZ polymers. Further, divalent calcium exerted strikingly different effects on the assembly of *Ec*FtsZ and *Mtb*FtsZ. Divalent calcium strongly enhanced the assembly of *Ec*FtsZ and promoted bundling and stability of the protofilaments. In contrast, it had no detectable effect on the assembly of *Mtb*FtsZ. *In vitro*, divalent calcium bound to *Ec*FtsZ with much stronger affinity than to *Mtb*FtsZ and significantly affected the secondary structure of *Ec*FtsZ whereas it did not cause any detectable change in the secondary structure of *Mtb*FtsZ. The results suggested that the assembly characteristics of *Ec*FtsZ and *Mtb*FtsZ are different and indicated that the assembly dynamics of these proteins are regulated by different mechanisms.

Key words: FtsZ assembly, bundling of protofilaments, polymer stability, GTPase activity, calcium.

Abbreviations: *Ec*FtsZ, *Escherichia coli* FtsZ; GTP, guanosine-5′-triphosphate; *Mtb*FtsZ, *Mycobacterium tuberculosis* FtsZ.

FtsZ, a key bacterial cell division protein, is present in almost all of the prokaryotes (*1–3*). After the completion of DNA segregation, FtsZ polymerizes to form a ring like structure at the mid cell of bacteria. This ring is known as the cytokinetic 'Z-ring' and is highly dynamic in nature (*4*). At the time of division, the Z-ring constricts to divide the cell into two and subsequently FtsZ depolymerizes into monomers leading to the disappearance of the Z-ring (*5*). FtsZ is considered as prokaryotic homologue of eukaryotic tubulin (*6–8*). Further similar to tubulin, FtsZ can assemble into protofilamentous structure in a GTP dependent manner (*9*, *10*). Depending on the assembly conditions, protofilaments can further form pairs, bundles, sheets and tubes by lateral association (*11*). In addition, FtsZ monomers can also form small circles called mini-rings (*12*). Polymerization of FtsZ can be promoted by divalent calcium (*13–15*), monosodium glutamate (*13*), ruthenium red (*16*), polycationic DEAE-dextran and cationic phospholipids (*12*).

Mycobacterium tuberculosis is causative organism of deadly infectious disease tuberculosis. *Mycobacterium tuberculosis* is a Gram-positive aerobic bacterium, which divides slowly compared to many other fast growing bacteria like *Escherichia coli*. While most of the bacteria divide every 20–30 min, doubling time for *Mycobacterium* is almost 20–24 h. This difference in doubling time of *M. tuberculosis* from other bacteria may be partially attributed to cell division machinery, which mainly involves FtsZ and its accessory proteins. During the last two decades extensive studies have been performed in order to elucidate the structural and functional properties of FtsZ (*1–3*). Although literature is crowded with studies involving *E. coli* FtsZ (*Ec*FtsZ), there are very few studies performed on the assembly properties of *M. tuberculosis* FtsZ (*Mtb*FtsZ). A previous report using 90° light scattering showed that the polymerization of *Mtb*FtsZ is very slow compared to the *Ec*FtsZ (*17*). In the present study, we wanted to probe the similarities and differences between the assembly properties of *Ec*FtsZ and *Mtb*FtsZ using several complimentary techniques.

Use of different techniques provided interesting insights on the assembly characteristics of the two FtsZ proteins. In addition, we also found that divalent calcium exerted differential effects on the assembly characteristics of *Ec*FtsZ and *Mtb*FtsZ. Consistent with previous studies (*13*, *15*, *18*); divalent calcium was found to strongly promote the assembly and bundling of *Ec*FtsZ. In contrast, divalent calcium had no noticeable effect on the assembly characteristics of *Mtb*FtsZ. The differential

*To whom correspondence should be addressed. Tel: +91-22-2576-7838, Fax: +91-22-2572-3480, E-mail: panda@iitb.ac.in

© The Authors 2009. Published by Oxford University Press on behalf of the Japanese Biochemical Society. All rights reserved.

Downloaded from http://jb.oxfordjournals.org/ at Islamic Azad University on September 28, 2012

effects of calcium on the assembly of *Ec*FtsZ and *Mtb*FtsZ may be explained considering weaker calcium binding affinity of *Mtb*FtsZ as compared to that of *Ec*FtsZ.

MATERIALS AND METHODS

Materials—N-2-Hydroxyethylpiperazine-N′-2-ethane-sulphonic acid (HEPES), guanosine-5′-triphosphate (GTP) were purchased from Sigma Chemical Company. 1-Anilinonaphthalene-8-sulphonic acid (ANS) was purchased from Molecular probes, USA and ammonium sulphate was from Merck. All other reagents used were of analytical grade.

Isolation and Purification of MtbFtsZ and EcFtsZ—*Mtb*FtsZ and *Ec*FtsZ proteins were over expressed in *E. coli* and purified as described recently (*19*, *20*). FtsZ concentration was measured by the method of Bradford (*21*) using BSA as a standard and stored at −80°C. The purity of FtsZ was estimated to be ∼98% from a Coomassie blue stained sodium dodecyl sulphate polyacrylamide gel electrophoresis.

Light Scattering Assay—FtsZs, both *Ec*FtsZ and *Mtb*FtsZ, were mixed with different concentrations of divalent calcium in 25 mM HEPES buffer, pH 6.5, 50 mM KCl and 5 mM $MgCl_2$ (buffer A) on ice. After addition of 1 mM GTP, the assembly milieu was immediately placed in a cuvette at 37°C. The polymerization reaction was followed by monitoring 90° light scattering at 500 nm, using a JASCO 6500 fluorescence spectrophotometer.

Sedimentation Assay—*Ec*FtsZ or *Mtb*FtsZ (6 μM) was polymerized in buffer A containing 1 mM GTP in the absence and presence of different concentrations (2–15 mM) of $CaCl_2$ for 30 min at 37°C. The polymers were collected by centrifugation at 227,000*g* for 30 min at 30°C. The protein concentration in the supernatant was measured by the Bradford method using BSA as a standard. Polymerized amount of FtsZ was determined by subtracting the supernatant concentration from the total protein concentration.

Electron Microscopy—The effects of divalent calcium on the assembly of *Ec*FtsZ or *Mtb*FtsZ were analysed by transmission electron microscopy (*19*, *22*). Briefly, FtsZ (6 μM) in buffer A in the absence and presence of 10 mM calcium was polymerized in the presence of GTP at 37°C for 30 min. The FtsZ polymers in the samples were fixed with warmed 0.5% glutaraldehyde for 5 min. FtsZ polymeric suspension (50 μl) were placed on the carbon-coated copper grids (300 mesh size) and then blotted dry. The grids were subsequently subjected to negative staining by 2% uranyl acetate solution and air-dried. The samples were examined using a FEI Tecnai-G^2 12 electron microscope.

Measurement of the GTPase Activity of FtsZ—The effect of divalent calcium on the GTPase activity of FtsZ was analysed by a standard malachite green ammonium molybdate assay (*23*) as described recently (*19*). Briefly, FtsZ (6 μM) in buffer A was mixed with different concentrations of divalent calcium on ice and 1 mM GTP was added to each of the reaction mixtures. The reaction mixtures were immediately transferred to 37°C and incubated for different time spans. The hydrolysis reaction was quenched at desired time intervals by adding 10% (v/v) 7 M perchloric acid. The quenched reaction mixtures were kept on ice until all the time points were collected. Then, the reaction mixtures were kept at room temperature for 10 min. Twenty microlitres of the reaction mixture were incubated with 900 μl of freshly prepared malachite green ammonium molybdate solution (0.045% malachite green, 4.2% ammonium molybdate and 0.02% Triton X-100) at room temperature for 30 min and the phosphate ions released were determined by measuring the absorbance of samples at 650 nm. An appropriate blank reading was subtracted from experimental data. A phosphate standard curve was prepared using sodium phosphate.

Stability of FtsZ Polymers in the Presence of Calcium—*Ec*FtsZ or *Mtb*FtsZ (30 μM) was polymerized in buffer A with 1 M glutamate and 1 mM GTP at 37°C for 30 min. The polymer suspension was then diluted 30 times to reach a final FtsZ concentration of 1 μM in warm HEPES buffer without or with different concentrations of divalent calcium (*16*). The diluted polymeric suspensions were kept at 37°C for another 5 min. Polymers were sedimented at 227,000*g* for 30 min at 30°C. The percent of total FtsZ pelleted in the absence and presence of different concentrations of divalent calcium was determined by subtracting the supernatant protein concentration from the total protein concentration.

Determination of Dissociation Constant of the Calcium–FtsZ Interaction—FtsZ was incubated without or with different concentrations of divalent calcium in 25 mM HEPES buffer at 25°C for 30 min. Then, 50 μM ANS was added to the reaction mixtures and incubated for an additional 30 min at 25°C. The fluorescence measurements were taken using 360 nm as an excitation wavelength. The increased FtsZ–ANS fluorescence at 470 nm upon binding to calcium was used to determine the dissociation constant (K_d) of the FtsZ and calcium interaction using the following equation:

$$\Delta F = \Delta F_{max}\, L/(K_d + L)$$

where ΔF is change in the fluorescence intensity of the FtsZ-ANS upon binding to calcium and was calculated by subtracting the fluorescence intensity of FtsZ–ANS in the absence of calcium from the fluorescence intensity of FtsZ–ANS in the presence of different concentrations of calcium, ΔF_{max} is the maximum change in the fluorescence intensity of FtsZ–ANS when it was fully saturated with calcium and L is the concentration of divalent calcium. The fluorescence intensity of FtsZ–ANS complex was calculated by subtracting the fluorescence intensity of free ANS from the fluorescence intensity of ANS in the presence of FtsZ. The ΔF_{max} values of 45 ± 6 and 13 ± 1.3 were calculated for *Ec*FtsZ and *Mtb*FtsZ, respectively by the GraphPad Prism 5 software. The data were statistically analysed and curve fitted using GraphPad Prism 5 software.

Circular Dichroism Spectroscopy Studies—FtsZ (4 μM) was incubated without or with different concentrations of divalent calcium at 25°C for 1 h. The far-UV circular dichroism (CD) spectra were monitored over the wavelength range of 200–250 nm using a 0.1-cm path length

Downloaded from http://jb.oxfordjournals.org/ at Islamic Azad University on September 28, 2012

cuvette with help of a JASCO J810 spectropolarimeter. A spectral bandwidth of 10 nm and time constant of 1 s were used for all measurements. Each spectrum was recorded using an average of five scans.

RESULTS

Polymerization of EcFtsZ and MtbFtsZ—Consistent with the earlier study (*17*), we found that the assembly of *Mtb*FtsZ occurred at a much slower rate than that of *Ec*FtsZ (Fig. 1A). For example, the light scattering intensity of *Ec*FtsZ assembly reached the maximum value in 50 s, whereas the light scattering intensity of *Mtb*FtsZ assembly attained the maximum value after ~900 s of assembly. In contrast, *Mtb*FtsZ found to produce more sedimentable polymers than *Ec*FtsZ (Fig. 1B). The results suggested that the assembly rate of *Mtb*FtsZ was much slower than that of the *Ec*FtsZ, while *Mtb*FtsZ polymers were efficiently pelleted (Fig. 1A and B).

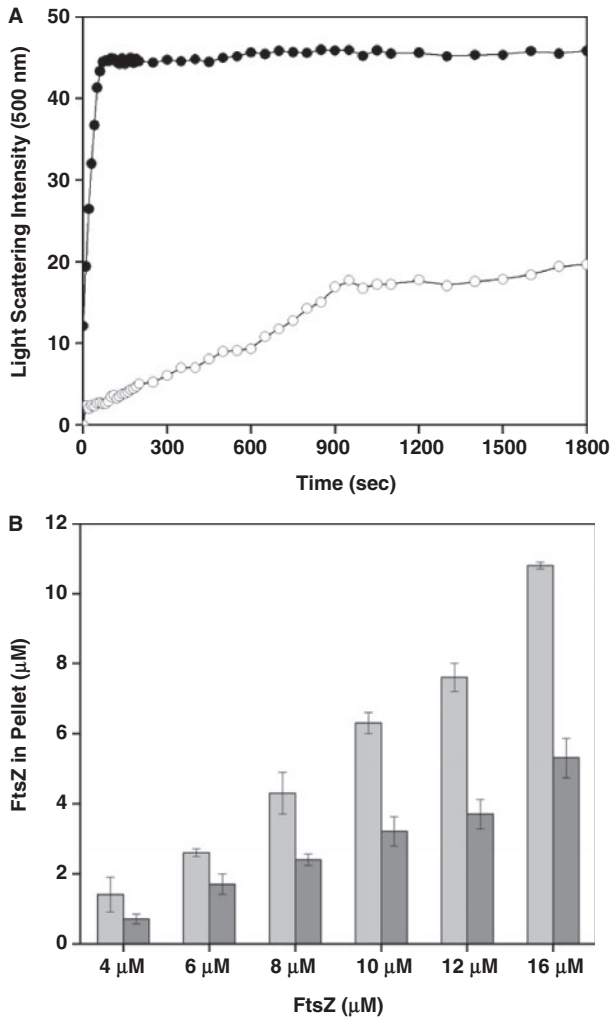

Fig. 1. **Assembly dynamics of FtsZ.** (A) *Ec*FtsZ (closed circle) and *Mtb*FtsZ (open circle) (15 μM) were polymerized in the presence of 25 mM HEPES buffer pH 6.5, 50 mM KCl, 5 mM $MgCl_2$ and 1 mM GTP at 37°C for 30 min. The rate and extent of polymerization was monitored by 90° light scattering for 30 min. (B) Polymerized mass of *Ec*FtsZ (dark grey bars) or *Mtb*FtsZ (light grey bars) proteins was determined by sedimentation assay. Different concentrations of FtsZ proteins were polymerized in buffer A for 30 min and the polymers were collected by centrifugation at 227,000*g* for 30 min at 30°C.

Further, *Ec*FtsZ and *Mtb*FtsZ were polymerized for 30 min. Then, 0.1% glutaraldehyde was added to the preformed polymers and the polymers were collected by centrifugation. Cross-linking the FtsZ polymers with glutaraldehyde caused a significant increase in the sedimentable polymeric mass for *Ec*FtsZ but it did not change the polymeric mass of *Mtb*FtsZ. For example, $28.2 \pm 2.4\%$ and $52.5 \pm 2.5\%$ of *Ec*FtsZ were found as polymers without or with cross-linking *Ec*FtsZ polymers using glutaraldehyde whereas 61 ± 2.1 and $63 \pm 2.2\%$ of *Mtb*FtsZ were sedimented without or with glutaraldehyde, respectively. The results suggested that *Ec*FtsZ polymers could disassemble during centrifugation.

Effects of Calcium on FtsZ Polymerization—Divalent calcium is known to promote the assembly and bundling of *Ec*FtsZ protofilaments (*13*, *15*, *18*). High concentration of *Ec*FtsZ is also known to assemble efficiently and to form extensive bundles; therefore, we used low concentration (6 μM) of FtsZ to determine the effects of calcium on the assembly and bundling of FtsZ. As observed previously (*13*, *15*, *18*), divalent calcium was found to remarkably increase the light scattering intensity of *Ec*FtsZ (Fig. 2A). For example, 10 mM calcium increased the light scattering intensity of *Ec*FtsZ assembly by ~20-fold than that of the control (in the absence of calcium), indicating that divalent calcium promotes the assembly and bundling of *Ec*FtsZ protofilaments. In contrast to the strong effects of divalent calcium on the assembly of *Ec*FtsZ, it had no discernible effect on the assembly of *Mtb*FtsZ. For example, the light scattering intensity of *Mtb*FtsZ assembly after 30 min of assembly in the absence and presence of 5 and 10 mM calcium were almost similar (Fig. 2B).

Further, to compare the effects of divalent calcium on the assembly of *Ec*FtsZ and *Mtb*FtsZ, the assembly kinetics of FtsZ was first monitored in the absence of calcium for 15 min. After 15 min of assembly, 10 mM calcium was added to the reaction milieu and the assembly kinetics was further monitored for an additional 30 min. The magnitude of light scattering intensity for the assembly of *Ec*FtsZ increased strikingly upon the addition of divalent calcium (Fig. 2C). In contrast, there was a minimal increase in the light scattering signal when 10 mM calcium was added to the *Mtb*FtsZ assembly milieu (Fig. 2C).

Divalent calcium increased the sedimentable polymerized mass of *Ec*FtsZ in a concentration-dependent manner (Fig. 3). For example, 25% of the total *Ec*FtsZ pelleted in the absence of calcium, whereas 30%, 50% and 87% of total *Ec*FtsZ sedimented in the presence of 2 mM, 4 mM and 8 mM of calcium, respectively. However, sedimentable polymer was not increased with further increasing the concentration of calcium (beyond 10 mM). In contrast, divalent calcium (2–15 mM) was found to have no detectable effect on the sedimentable polymer mass of *Mtb*FtsZ (Fig. 3). For example, 67% and 68% of the total *Mtb*FtsZ was polymerized in the absence and

Downloaded from http://jb.oxfordjournals.org/ at Islamic Azad University on September 28, 2012

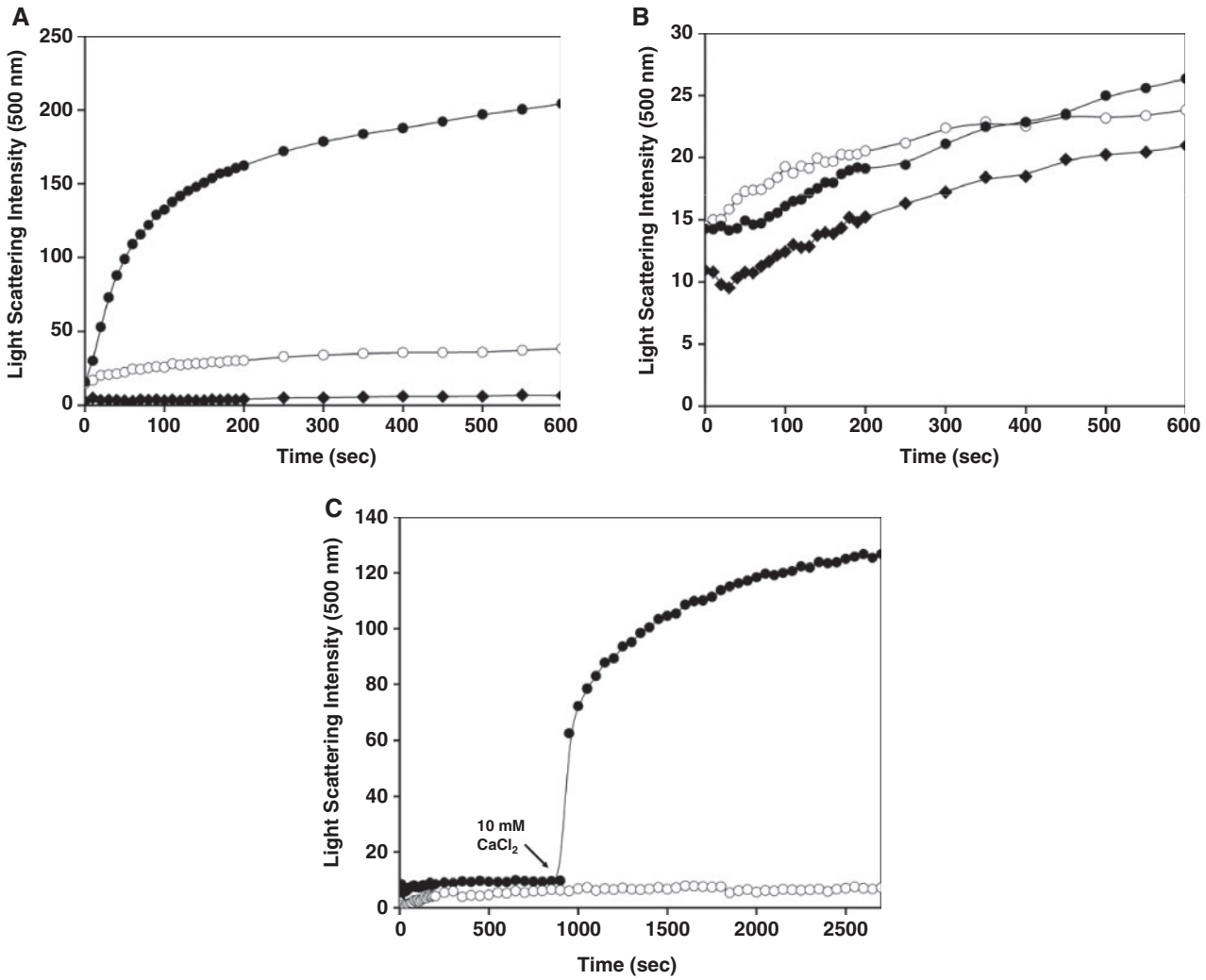

Fig. 2. **Effects of divalent calcium on the kinetics of FtsZ assembly.** *Ec*FtsZ or *Mtb*FtsZ (6 μM) was polymerized in the presence of 25 mM HEPES buffer pH 6.5, 50 mM KCl, 5 mM $MgCl_2$, 1 mM GTP and different concentrations of $CaCl_2$ at 37°C. The rate and extent of polymerization was monitored by 90° light scattering for 10 min. Shown are *Ec*FtsZ (A) and *Mtb*FtsZ (B) in the absence (filled diamond) and in the presence of 5 mM (open circle) and 10 mM (closed circle) $CaCl_2$. (C) Shows the light scattering traces of *Mtb*FtsZ (open circle) and *Ec*FtsZ (closed circle). Arrow depicts the addition of 10 mM calcium after 900 s of polymerization of FtsZ. Each experiment was performed four times.

presence of 8 mM of calcium, respectively, which was in resonance with the light scattering assay.

Under the conditions used, *Ec*FtsZ formed only few protofilaments in the absence of calcium and these protofilaments were thin (Fig. 4A). Average thickness of *Ec*FtsZ polymers increased in the presence of divalent calcium (Fig. 4B). For example, width of FtsZ polymers in the absence and presence of 10 mM divalent calcium were measured to be 13 ± 2.5 nm and 53 ± 11 nm, respectively. The results suggested that the significant enhancement of light scattering intensity of *Ec*FtsZ assembly in the presence of calcium was due to the combination of an increase in the polymerized mass and the bundling of FtsZ protofilaments. However, divalent calcium did not have any effect on the morphology of protofilaments and the extent of protofilaments bundling of *Mtb*FtsZ (Fig. 4C and D). For example, the protofilaments thickness of *Mtb*FtsZ in the absence and presence of calcium observed to be 19 ± 3 nm and 18 ± 5 nm, respectively.

GTPase Activity of MtbFtsZ was not Affected by Calcium—The GTPase activity of *Ec*FtsZ was strongly suppressed in the presence of 10 mM calcium (Fig. 5A). For example, after 30 min of hydrolysis reaction, 35 ± 1.3 mol and 8.2 ± 0.4 mol of inorganic phosphate released per mol of *Ec*FtsZ in the absence and presence of 10 mM calcium, respectively ($P < 0.01$). In addition, the rate of Pi released per *Ec*FtsZ molecule per minute was calculated to be 2.1 and 0.3 in the absence and presence of 10 mM calcium, respectively, suggesting that calcium strongly suppressed the GTP hydrolysis of *Ec*FtsZ. The rate of Pi released was found to be ~0.14 per minute per *Mtb*FtsZ molecule indicating that the GTPase activity of *Mtb*FtsZ is slow as compared to that of *Ec*FtsZ. In contrast to the strong inhibitory effects of the divalent calcium on the GTPase activity of *Ec*FtsZ,

Downloaded from http://jb.oxfordjournals.org/ at Islamic Azad University on September 28, 2012

the GTPase activity of *Mtb*FtsZ was not significantly inhibited by divalent calcium (Fig. 5B). For example, after 30 min of hydrolysis, phosphate released per mole of *Mtb*FtsZ were found to be 7.6 ± 1.8 and 7.0 ± 1.9 mol in the absence and presence of 10 mM calcium, respectively.

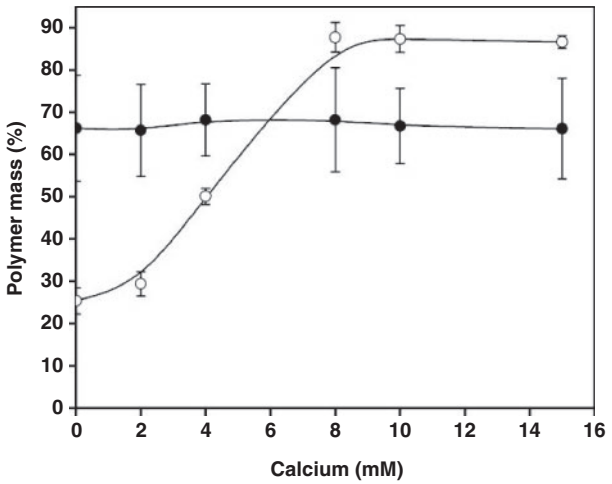

Fig. 3. **Effects of calcium on the polymerized mass of FtsZ.** FtsZ (6 μM) was polymerized in 25 mM HEPES buffer pH 6.5, 50 mM KCl, 5 mM $MgCl_2$, 1 mM GTP in the absence and presence of different concentration of $CaCl_2$ at 37°C for 30 min as described in MATERIALS AND METHODS section. The polymers were collected by centrifugation at 227,000*g* for 30 min. The polymeric mass of *Ec*FtsZ and *Mtb*FtsZ was determined by subtracting the supernatant protein concentration from the total protein concentration. Shown are the percent polymer mass of *Ec*FtsZ (open circle) and *Mtb*FtsZ (closed circle) as a function of increasing concentration of calcium. The experiment was performed four times.

Dilution-induced Disassembly—The effect of calcium on the stability of the preformed FtsZ polymers was analysed using a dilution-induced disassembly assay (*13*, *16*). *Ec*FtsZ or *Mtb*FtsZ (30 μM) was polymerized in the presence of 1 M glutamate for 30 min at 37°C. The polymers formed were diluted 30 times in warm 25 mM HEPES buffer without or with different concentrations of calcium. After 5 min of incubation at 37°C the polymers were sedimented. The sedimented *Ec*FtsZ protein concentrations in the pellet were found to increase with increasing concentration of calcium (Fig. 6). For example, 10%, 17%, 25% and 32% of the total *Ec*FtsZ was pelleted in the presence of 2, 5, 7 and 10 mM of calcium, suggesting that divalent calcium protected *Ec*FtsZ polymers against dilution-induced disassembly. Under similar conditions, divalent calcium failed to protect the preformed *Mtb*FtsZ polymers against dilution-induced disassembly (Fig. 6). For example, 11% and 9% of *Mtb*FtsZ were pelleted under challenged conditions in the absence and presence of 10 mM divalent calcium. Similarly, divalent calcium could not prevent the dilution-induced disassembly of preformed *Mtb*FtsZ polymers when *Mtb*FtsZ was polymerized in the absence of glutamate, whereas it strongly prevented the dilution-induced disassembly of *Ec*FtsZ polymers under similar conditions (data not shown).

Determination of Dissociation Constant of Calcium Binding to FtsZ—It has been reported that divalent calcium increases the fluorescence of FtsZ bound ANS (*24*). Therefore, the binding of calcium to *Ec*FtsZ and *Mtb*FtsZ was monitored using the change of ANS fluorescence upon calcium binding (Fig. 7). The fluorescence intensities of *Ec*FtsZ–ANS complex in the absence and presence of 10 mM calcium was observed to be 23.6 ± 3.5 and

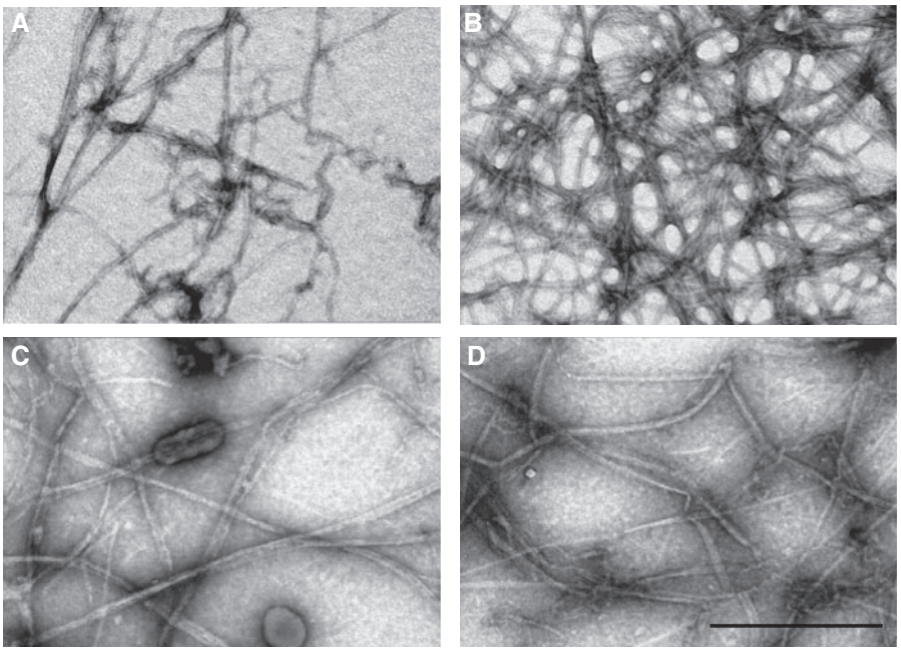

Fig. 4. **Differential effects of divalent calcium on *Ec*FtsZ and *Mtb*FtsZ polymers.** FtsZ (6 μM) was polymerized in 25 mM HEPES buffer, pH 6.5, containing 50 mM KCl, 5 mM $MgCl_2$ and 1 mM GTP at 37°C in the absence and presence of 10 mM calcium for 30 min. Shown are electron micrographs of *Ec*FtsZ and *Mtb*FtsZ polymers formed in the absence (A and C) and presence of 10 mM (B and D) calcium, respectively. The scale bar is 500 nm.

Downloaded from http://jb.oxfordjournals.org/ at Islamic Azad University on September 28, 2012

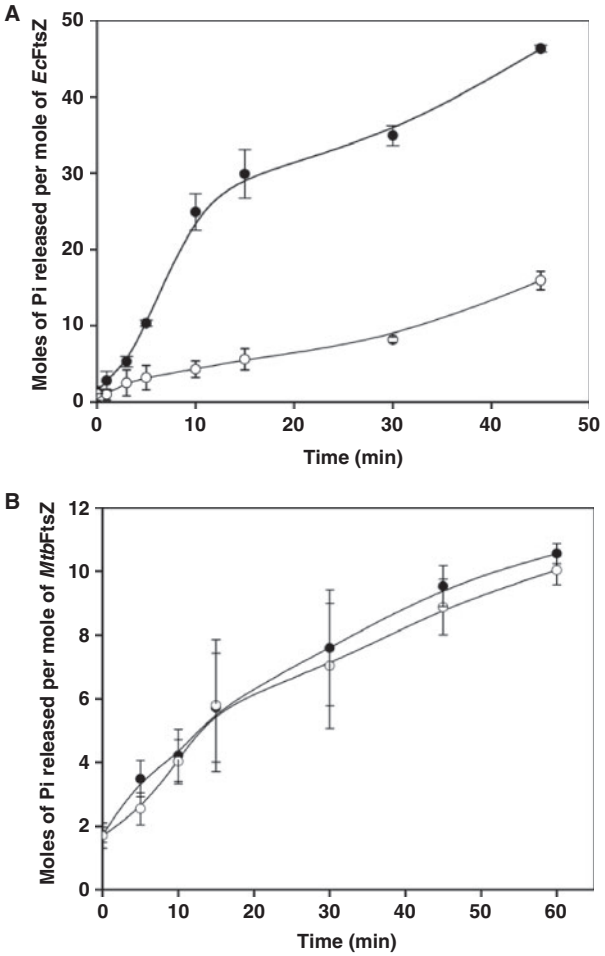

Fig. 5. **Effect of calcium on the GTPase activity of *Ec*FtsZ and *Mtb*FtsZ.** FtsZ (6 μM) was incubated in 25 mM HEPES buffer pH 6.5, 50 mM KCl, 5 mM $MgCl_2$ and 1 mM GTP in the absence and presence of 10 mM calcium. Shown are the moles of Pi released per mol of *Ec*FtsZ (A) and *Mtb*FtsZ (B) in the absence (closed circle) and presence (open circle) of 10 mM calcium.

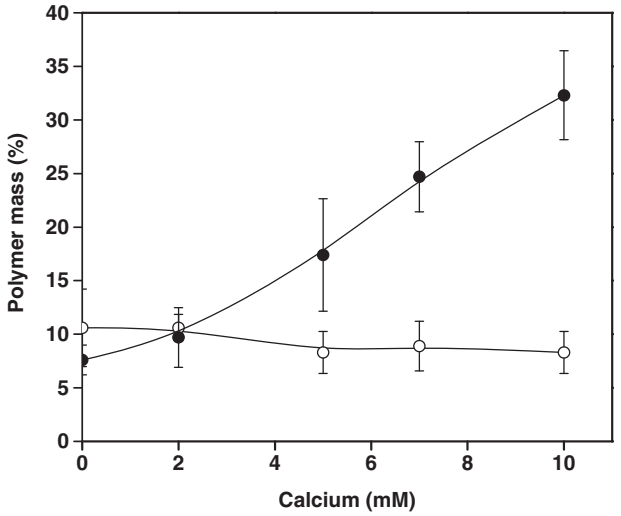

Fig. 6. **Effect of calcium on the stabilization of *Ec*FtsZ and *Mtb*FtsZ against dilution-induced disassembly.** FtsZ (30 μM) was polymerized in 25 mM HEPES buffer pH 6.5, 50 mM KCl, 5 mM $MgCl_2$, 1 mM GTP and 1 M glutamate as described in MATERIALS AND METHODS section. The polymer suspension was then diluted 30 times to reach a final FtsZ concentration of 1 μM in warm HEPES buffer without or with different concentrations of calcium. Shown are the percent polymer mass of *Ec*FtsZ (closed circle) and *Mtb*FtsZ (open circle) pelleted in the absence or presence of different concentrations of calcium.

61 ± 1.2 at 470 nm, respectively (Fig. 7A). Under the similar reaction conditions, the fluorescence intensities of *Mtb*FtsZ–ANS complex were observed to be 10.8 ± 0.5 and 18.9 ± 1.6, in the absence and presence of 10 mM calcium, respectively (Fig. 7B). The dissociation constant of calcium for *Ec*FtsZ and *Mtb*FtsZ were calculated to be 1.1 ± 0.2 mM (Fig. 7A, inset) and 6.9 ± 0.3 mM (Fig. 7B, inset), respectively. The finding suggested that divalent calcium binds to *Ec*FtsZ with higher affinity than to *Mtb*FtsZ. The dissociation constant of the interaction between divalent calcium and *Mtb*FtsZ at pH 8 was determined to be 3.5 ± 0.4 mM, suggesting that the binding affinity of divalent calcium with *Mtb*FtsZ increases upon increasing the pH of the reaction milieu (Fig. 7C).

Secondary Structure Studies—To compare the effect of calcium on the secondary structure of *Ec*FtsZ and *Mtb*FtsZ the far UV-CD spectra of FtsZ were monitored in the absence and presence of different concentrations of divalent calcium. There was a significant change in the far-UV CD spectra of *Ec*FtsZ with increasing concentration of calcium (Fig. 8A). For example, the CD signal (222 nm) of *Ec*FtsZ was increased by 7%, 16% and 21% in the presence of 2, 5 and 10 mM of calcium, respectively, suggesting that calcium altered the secondary structures of *Ec*FtsZ. The far-UV CD spectra of *Mtb*FtsZ did not change detectably in the presence of different concentrations of calcium, suggesting that calcium did not alter the secondary structure of *Mtb*FtsZ (Fig. 8B).

DISCUSSION

Consistent with the previous report (*17*), *Mtb*FtsZ was found to polymerize at a much slower rate than that of *Ec*FtsZ and also to hydrolyse GTP at much slower rate than *Ec*FtsZ. In contrast, *Mtb*FtsZ produced significantly higher sedimentable polymeric mass than *Ec*FtsZ. Higher sedimentable, polymerized mass of *Mtb*FtsZ than that of *Ec*FtsZ could be due to two reasons. *Ec*FtsZ polymers were smaller in size than *Mtb*FtsZ polymers; therefore, *Ec*FtsZ polymers were not efficiently precipitated. It was an unlikely possibility because the FtsZ polymers were precipitated using a very high centrifugal force (227,000 *g*). Alternatively, *Ec*FtsZ polymers are unstable as compared to *Mtb*FtsZ polymers. Therefore, it was possible to recover most of the *Mtb*FtsZ polymers by high-speed centrifugation, whereas highly dynamic *Ec*FtsZ polymers were depolymerized fast under high centrifugal force and led to the lesser recovery of polymers. To test whether *Ec*FtsZ

Downloaded from http://jb.oxfordjournals.org/ at Islamic Azad University on September 28, 2012

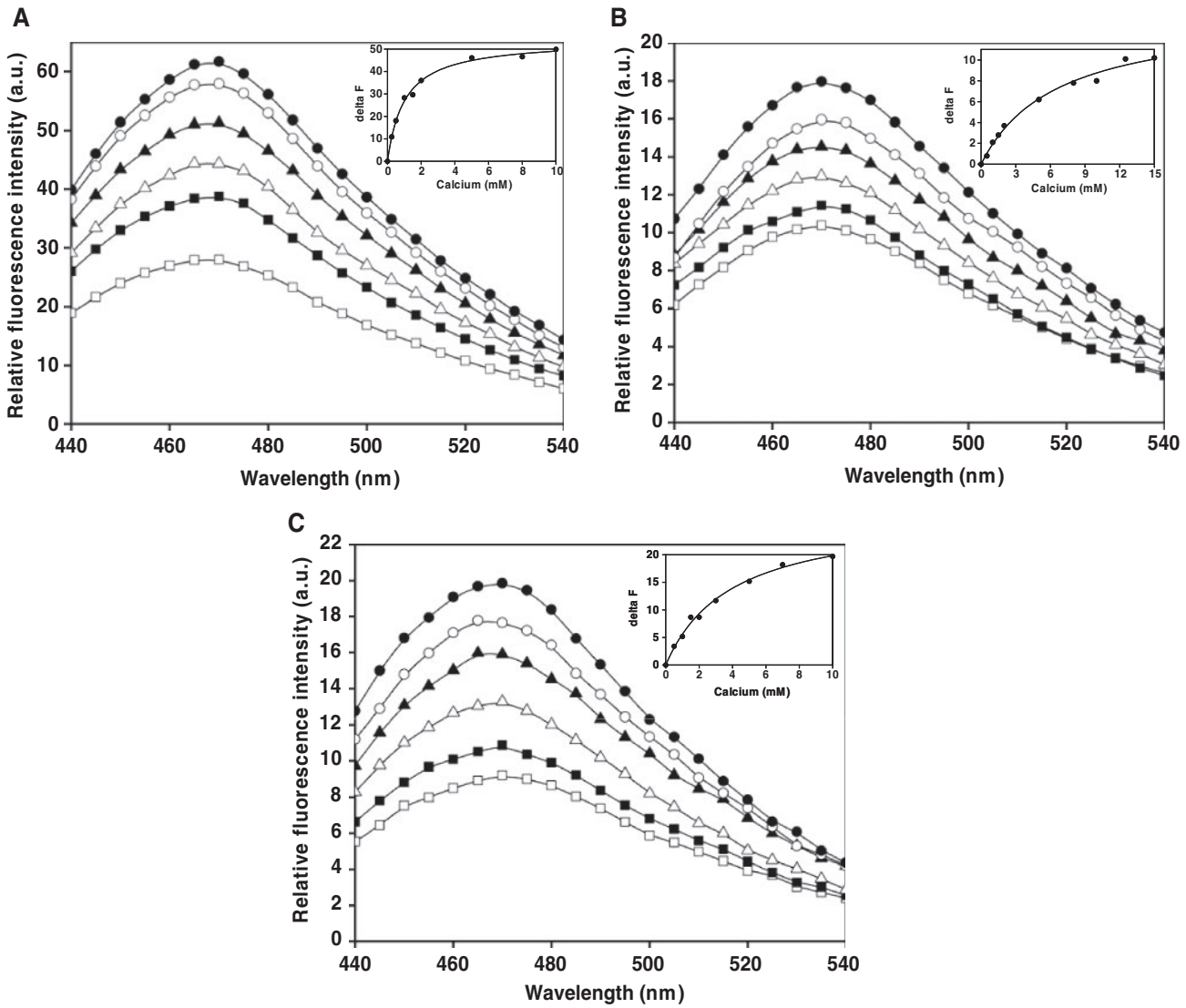

Fig. 7. **Binding of divalent calcium to FtsZ.** Shown are the emission spectra of *Ec*FtsZ (A) and *Mtb*FtsZ (B) at pH 6.5 and the emission spectra of *Mtb*FtsZ at pH 8.0 (C) in the absence (open square) and presence of 0.5 mM (closed square), 1 mM (open triangle), 2 mM (closed triangle), 5 mM (open circle) and 10 mM (closed circle) calcium. The inset in each panel shows the change in the fluorescence intensity of FtsZ–ANS complex in the presence of different concentrations of divalent calcium.

protofilaments were depolymerized during centrifugation, preformed *Ec*FtsZ polymers were fixed using 0.1% glutaraldehyde prior to the centrifugation. It was possible to recover ~2-fold higher amount of polymerized *Ec*FtsZ in the presence of glutaraldehyde as compared to the control (in the absence of glutaraldehyde fixing). Under similar assembly conditions *Mtb*FtsZ did not show any change in the polymer mass without or with 0.1% glutaraldehyde suggesting that *Mtb*FtsZ polymers do not depolymerize and that these polymers are more stable than the *Ec*FtsZ polymers. Consistent with this argument, *Mtb*FtsZ was shown to depolymerize slowly (*17*). Under similar assembly conditions, the mean width of *Ec*FtsZ protofilaments (13 ± 2.5 nm) was found to be significantly thinner than that of the *Mtb*FtsZ (19 ± 3 nm) ($P < 0.001$) suggesting that *Mtb*FtsZ polymers contained one extra protofilament compared to *Ec*FtsZ. The extra protofilament might provide the stability for *Mtb*FtsZ polymers. The large light scattering signal in the presence of high concentration of *Ec*FtsZ could be due to large bundles (Fig. 1), while the weak light scattering signal of *Mtb*FtsZ assembly indicated that *Mtb*FtsZ may not produce large bundles under similar conditions.

Consistent with previous reports (*13*, *15*, *16*, *18*), we also found that divalent calcium strongly enhanced the light scattering intensity, increased polymer mass, induced bundling of FtsZ protofilaments and reduced GTPase activity of *Ec*FtsZ. Though it has been shown that calcium is not essential for FtsZ polymerization as such (*18*), the effect of calcium on the Z-ring formation and cell division cannot be ruled out. The effects of calcium on FtsZ assembly were observed in millimolar concentrations of calcium ions. Although this concentration range of calcium is quite high for *in vivo* condition,

Downloaded from http://jb.oxfordjournals.org/ at Islamic Azad University on September 28, 2012

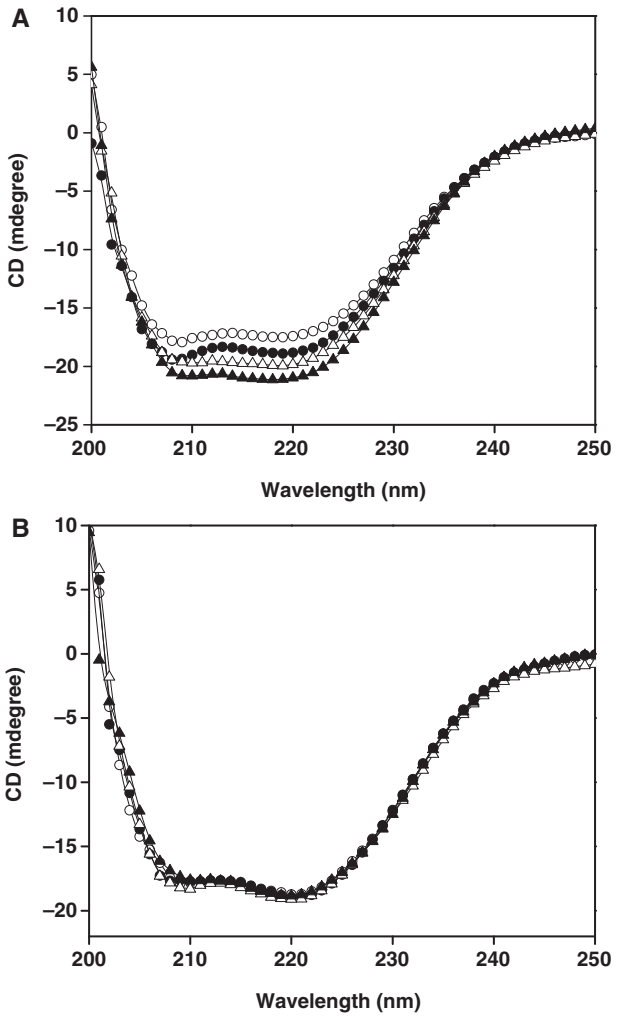

Fig. 8. **Effect of calcium on the secondary structure of *Ec*FtsZ and *Mtb*FtsZ.** Shown are the far-UV CD spectra of *Ec*FtsZ (A) and *Mtb*FtsZ (B) in the absence (open circle) and presence of 2 mM (closed circle), 5 mM (open triangle) and 10 mM (closed triangle) calcium.

it has been estimated that a transient mobilization of all calcium (bound to DNA, membranes, *etc*.) inside *E. coli* cells could raise the calcium concentration to millimolar levels (*15*, *25*). Another study showed that in actively dividing *E. coli* cells the total calcium concentration is almost 20-fold higher, compared to that of the non-dividing cells where it is estimated to be 1.5 mmol/kg (*26*). Therefore, it has been hypothesized that there could be a spatially regulated import of calcium resulting in the transient increase of the calcium concentration during cell division (*26*). The high calcium concentrations are in accordance to the concentrations that are required for the FtsZ assembly *in vitro*. It has been suggested that calcium ions act as a possible trigger for the major cell cycle events in bacteria, including cytokinesis (*27*). Several of the FtsZ regulatory proteins including ZipA (in *E. coli*, *28*), and ZapA (in *Bacillus subtilis*, *29*) are known to stabilize Z-ring formation and these proteins are also shown to promote the assembly and bundling of FtsZ *in vitro*. It is tempting to speculate that divalent calcium may play similar role in FtsZ polymerization and Z-ring formation in bacteria. In contrast, divalent calcium did not have a detectable effect on the assembly properties of *Mtb*FtsZ suggesting that assembly dynamics of *Ec*FtsZ and *Mtb*FtsZ may be regulated differently.

Recently, it has been shown that *Mtb*FtsZ formed two stranded filaments and small bundles along with one stranded filaments in the presence of 10 mM calcium at pH 7.7 (*30*). This apparent discrepancy from the results presented in this study might be due to an increase in the binding affinity of divalent calcium for FtsZ at higher pH. Consistent with this idea, the binding affinity of calcium for *Mtb*FtsZ at pH 8 was found to increase by ~2-fold as compared to the binding affinity at pH 6.5 (Fig. 7B and C). Generally, the binding affinity of divalent calcium to proteins has been found to increase with increasing pH (*31*, *32*). Therefore, divalent calcium might induce limited bundling of FtsZ protofilaments at the elevated pH. Besides, Chen *et al*. (*30*) also did not report strong bundling of *Mtb*FtsZ protofilaments in the presence of 10 mM calcium. Under similar conditions, divalent calcium strongly increased the bundling of *Ec*FtsZ protofilaments (average thickness of the protofilaments increased from 13 ± 2.5 nm and 53 ± 11 nm) and stabilized the protofilaments, whereas divalent calcium had no discernible effect on the assembly of *Mtb*FtsZ.

In case of *Ec*FtsZ, calcium induces the bundle formation, which involves lateral association of the protofilaments. Under the experimental conditions used, the sedimentable polymerized mass of *Ec*FtsZ increased with increasing concentration of divalent calcium (Fig. 3). A homology model of *Ec*FtsZ has been shown to have predominantly negatively charged surface (*33*). Divalent calcium might be helping in charge neutralization and thus, minimizing repulsion between two protofilaments leading to bundle formation. We analysed the surface charge distribution of *Mtb*FtsZ using APBS (*34*) and PyMol softwares (*35*). Interestingly, *Mtb*FtsZ also showed prevalence of negatively charged surface (data not shown). However, the polymerized mass of *Mtb*FtsZ remained unchanged in the absence or the presence of divalent calcium (up to 15 mM) indicating that either divalent calcium bound weakly to *Mtb*FtsZ protofilaments or it could not increase the interactions between *Mtb*FtsZ protofilaments (Fig. 3).

It has been suggested that an increase in hydrophobic forces may increase the lateral interactions between the protofilaments and thereby, induce bundling of FtsZ protofilaments (*20*). We found that divalent calcium increased the fluorescence of FtsZ–ANS complex indicating that it might alter the hydrophobic surfaces of both the FtsZ. However, divalent calcium increased the fluorescence of *Ec*FtsZ–ANS strongly as compared to that of the *Mtb*FtsZ–ANS indicating that calcium exerted stronger effects on the conformation of *Ec*FtsZ than that of the *Mtb*FtsZ. The mode of interaction of divalent calcium with *Ec*FtsZ and *Mtb*FtsZ might be different. Divalent calcium also altered the secondary structure of *Ec*FtsZ and it had no discernable effect on the secondary structure of *Mtb*FtsZ. The differential mode of binding of divalent calcium to *Ec*FtsZ and *Mtb*FtsZ may also

Downloaded from http://jb.oxfordjournals.org/ at Islamic Azad University on September 28, 2012

be due to the different sort of stacking units because *Ec*FstZ exists in monomeric form under non assembly conditions while *Mtb*FtsZ exists as dimer (*36*). *Ec*FtsZ monomers stack longitudinally during protofilament formation and these protofilaments are thought to further associate laterally to form different polymeric structures like bundles, sheets and tubes (*12*). Whereas two subunits of *Mtb*FtsZ associate laterally to form an arc-shaped dimer, then, there may be lateral or longitudinal expansion of these dimers to form polymeric structures (*36*). The difference in the mode of the binding of divalent calcium to *Ec*FtsZ and *Mtb*FtsZ may be one of the contributing factors for the differential effects of calcium on the assembly of two FtsZ proteins.

ACKNOWLEDGEMENTS

D.P. thanks Swarnajayanthi fellowship and R.J. thanks CSIR fellowship.

FUNDING

The Department of Science and Technology, Government of India (to D.P.).

CONFLICT OF INTEREST

None declared.

REFERENCES

1. Graumann, P.L. (2007) Cytoskeletal elements in bacteria. *Annu. Rev. Microbiol.* **61**, 589–618
2. Harry, E., Monahan, L., and Thompson, L. (2006) Bacterial cell division: the mechanism and its precison. *Int. Rev. Cytol.* **253**, 27–94
3. Margolin, W. (2005) FtsZ and the division of prokaryotic cells and organelles. *Nat. Rev. Mol. Cell Biol.* **6**, 862–871
4. Stricker, J., Maddox, P., Salmon, E.D., and Erickson, H.P. (2002) Rapid assembly dynamics of the Escherichia coli FtsZ-ring demonstrated by fluorescence recovery after photobleaching. *Proc. Natl Acad. Sci. USA* **99**, 3171–3175
5. Romberg, L. and Levin, P.A. (2003) Assembly dynamics of the bacterial cell division protein FTSZ: poised at the edge of stability. *Annu. Rev. Microbiol.* **57**, 125–154
6. Lowe, J. and Amos, L.A. (1998) Crystal structure of the bacterial cell-division protein FtsZ. *Nature* **391**, 203–206
7. Michie, K.A. and Lowe, J. (2006) Dynamic filaments of the bacterial cytoskeleton. *Annu. Rev. Biochem.* **75**, 467–492
8. van den, E.F., Amos, L., and Lowe, J. (2001) Bacterial ancestry of actin and tubulin. *Curr. Opin. Microbiol.* **4**, 634–638
9. Mukherjee, A. and Lutkenhaus, J. (1994) Guanine nucleotide-dependent assembly of FtsZ into filaments. *J. Bacteriol.* **176**, 2754–2758
10. Nogales, E., Downing, K.H., Amos, L.A., and Lowe, J. (1998) Tubulin and FtsZ form a distinct family of GTPases. *Nat. Struct. Biol.* **5**, 451–458
11. Lowe, J. and Amos, L.A. (2000) Helical tubes of FtsZ from Methanococcus jannaschii. *Biol. Chem.* **381**, 993–999
12. Erickson, H.P., Taylor, D.W., Taylor, K.A., and Bramhill, D. (1996) Bacterial cell division protein FtsZ assembles into protofilament sheets and minirings, structural homologs of tubulin polymers. *Proc. Natl Acad. Sci. USA* **93**, 519–523
13. Beuria, T.K., Krishnakumar, S.S., Sahar, S., Singh, N., Gupta, K., Meshram, M., and Panda, D. (2003) Glutamate-induced assembly of bacterial cell division protein FtsZ. *J. Biol. Chem.* **278**, 3735–3741
14. Lowe, J. and Amos, L.A. (1999) Tubulin-like protofilaments in Ca2+-induced FtsZ sheets. *EMBO J.* **18**, 2364–2371
15. Yu, X.C. and Margolin, W. (1997) Ca2+-mediated GTP-dependent dynamic assembly of bacterial cell division protein FtsZ into asters and polymer networks in vitro. *EMBO J.* **16**, 5455–5463
16. Santra, M.K., Beuria, T.K., Banerjee, A., and Panda, D. (2004) Ruthenium red-induced bundling of bacterial cell division protein, FtsZ. *J. Biol. Chem.* **279**, 25959–25965
17. White, E.L., Ross, L.J., Reynolds, R.C., Seitz, L.E., Moore, G.D., and Borhani, D.W. (2000) Slow polymerization of Mycobacterium tuberculosis FtsZ. *J. Bacteriol.* **182**, 4028–4034
18. Mukherjee, A. and Lutkenhaus, J. (1999) Analysis of FtsZ assembly by light scattering and determination of the role of divalent metal cations. *J. Bacteriol.* **181**, 823–832
19. Jaiswal, R., Beuria, T.K., Mohan, R., Mahajan, S.K., and Panda, D. (2007) Totarol inhibits bacterial cytokinesis by perturbing the assembly dynamics of FtsZ. *Biochemistry* **46**, 4211–4220
20. Santra, M.K. and Panda, D. (2007) Acid-induced loss of functional properties of bacterial cell division protein FtsZ: evidence for an alternative conformation at acidic pH. *Proteins* **67**, 177–188
21. Bradford, M.M. (1976) A rapid and sensitive method for the quantitation of microgram quantities of protein utilizing the principle of protein-dye binding. *Anal. Biochem.* **72**, 248–254
22. Jaiswal, R. and Panda, D. (2008) Cysteine 155 plays an important role in the assembly of Mycobacterium tuberculosis FtsZ. *Protein Sci.* **17**, 846–854
23. Geladopoulos, T.P., Sotiroudis, T.G., and Evangelopoulos, A.E. (1991) A malachite green colorimetric assay for protein phosphatase activity. *Anal. Biochem.* **192**, 112–116
24. Yu, X.C. and Margolin, W. (1998) Inhibition of assembly of bacterial cell division protein FtsZ by the hydrophobic dye 5,5′-bis-(8-anilino-1-naphthalenesulfonate). *J. Biol. Chem.* **273**, 10216–10222
25. Holland, I.B., Jones, H.E., Campbell, A.K., and Jacq, A. (1999) An assessment of the role of intracellular free Ca2+ in *E. coli*. *Biochimie* **81**, 901–907
26. Chang, C.F., Shuman, H., and Somlyo, A.P. (1986) Electron probe analysis, X-ray mapping, and electron energy-loss spectroscopy of calcium, magnesium, and monovalent ions in log-phase and in dividing Escherichia coli B cells. *J. Bacteriol.* **167**, 935–939
27. Norris, V., Seror, S.J., Casaregola, S., and Holland, I.B. (1988) A single calcium flux triggers chromosome replication, segregation and septation in bacteria: a model. *J. Theor. Biol.* **134**, 341–350
28. Hale, C.A., Rhee, A.C., and de Boer, P.A. (2000) ZipA-induced bundling of FtsZ polymers mediated by an interaction between C-terminal domains. *J. Bacteriol.* **182**, 5153–5166
29. Gueiros-Filho, F.J. and Losick, R. (2002) A widely conserved bacterial cell division protein that promotes assembly of the tubulin-like protein FtsZ. *Genes Dev.* **16**, 2544–2556
30. Chen, Y., Anderson, D.E., Rajagopalan, M., and Erickson, H.P. (2007) Assembly dynamics of Mycobacterium tuberculosis FtsZ. *J. Biol. Chem.* **282**, 27736–27743
31. Wallace, G.W. and Satterlee, L.D. (1978) Protein-calcium binding and its effect on several food protein properties, molecular weights and isoelectric points. *J. Food Biochem.* **1**, 367–384
32. Pacheco, M.T., Carraro, F., and Sgarbieri, V.C. (1999) Study of calcium binding to different preparations of yeast

Downloaded from http://jb.oxfordjournals.org/ at Islamic Azad University on September 28, 2012

(Saccharomyces cerevisiae) protein by using an ion selective electrode. *Food Chem.* **66**, 249–252
33. Beuria, T.K., Shah, J.H., Santra, M.K., Kumar, V., and Panda, D. (2006) Effects of pH and ionic strength on the assembly and bundling of FtsZ protofilaments: a possible role of electrostatic interactions in the bundling of protofilaments. *Int. J. Biol. Macromol.* **40**, 30–39
34. Baker, N.A., Sept, D., Joseph, S., Holst, M.J., and McCammon, J.A. (2001) Electrostatics of nanosystems: application to microtubules and the ribosome. *Proc. Natl Acad. Sci. USA* **98**, 10037–10041
35. DeLano, W.L. (2002) The PyMOL Molecular Graphics System (2002) on World Wide Web http://www.pymol.org, accessed date 17 July, 2008
36. Leung, A.K., Lucile, W.E., Ross, L.J., Reynolds, R.C., DeVito, J.A., and Borhani, D.W. (2004) Structure of Mycobacterium tuberculosis FtsZ reveals unexpected, G protein-like conformational switches. *J. Mol. Biol.* **342**, 953–970

Downloaded from http://jb.oxfordjournals.org/ at Islamic Azad University on September 28, 2012